© 2014. Published by The Company of Biologists Ltd | Development (2014) 141, 3159-3164 doi:10.1242/dev.108498

RESEARCH REPORT

Dual roles for Id4 in the regulation of estrogen signaling in the mammary gland and ovary

Sarah A. Best[1,2], Karla J. Hutt[3,4], Nai Yang Fu[1,2], François Vaillant[1,2], Seng H. Liew[3], Lynne Hartley[1], Clare L. Scott[1,5,6], Geoffrey J. Lindeman[1,5,6] and Jane E. Visvader[1,2,*]

ABSTRACT

The HLH transcriptional regulator Id4 exerts important roles in different organs, including the neural compartment, where Id4 loss usually results in early lethality. To explore the role of this basally restricted transcription factor in the mammary gland, we generated a *cre*-inducible mouse model. MMTV- or K14-*cre*-mediated deletion of *Id4* led to a delay in ductal morphogenesis, consistent with previous findings using a germ-line knockout mouse model. A striking increase in the expression of ERα (Esr1), PR and FoxA1 was observed in both the basal and luminal cellular subsets of *Id4*-deficient mammary glands. Together with chromatin immunoprecipitation of Id4 on the *Esr1* and *Foxa1* promoter regions, these data imply that Id4 is a negative regulator of the ERα signaling axis. Unexpectedly, examination of the ovaries of targeted mice revealed significantly increased numbers of secondary and antral follicles, and reduced Id4 expression in the granulosa cells. Moreover, expression of the cascade of enzymes that are crucial for estrogen biosynthesis in the ovary was decreased in *Id4*-deficient females and uterine weights were considerably lower, indicating impaired estrogen production. Thus, compromised ovarian function and decreased circulating estrogen likely contribute to the mammary ductal defects evident in *Id4*-deficient mice. Collectively, these data identify Id4 as a novel regulator of estrogen signaling, where Id4 restrains ERα expression in the basal and luminal cellular compartments of the mammary gland and regulates estrogen biosynthesis in the ovary.

KEY WORDS: Mammary gland, ID proteins, Estrogen, Ovary, Mouse

INTRODUCTION

The Id family of helix-loop-helix proteins comprises four members (Id1-Id4) that have emerged as important regulators of the balance between proliferation and differentiation in a number of different developmental systems (Lasorella et al., 2014; Sikder et al., 2003). Id proteins lack a DNA-binding motif and appear to function by sequestering basic-HLH factors from dimerizing with their partner proteins and thus preventing them from binding DNA to regulate transcription. Id4 is of particular interest because it has been shown to be important for development of the neural system, mammary gland and prostate using a germline knockout model. Only 20% of mice survive on an *Id4*-null background, following a high proportion of embryonic and post-partum lethality resulting from severe brain and neuronal abnormalities (Bedford et al., 2005; Yun et al., 2004). In the male reproductive system, Id4 loss results in significantly reduced seminal vesicle size, prostatic intraepithelial neoplasia (PIN) lesions and sterility (Sharma et al., 2013), while a recent study in the mammary gland has shown that Id4 governs ductal elongation and branching via the Id4 target p38MAPK (Dong et al., 2011). In breast epithelial cells, Id4 negatively controls expression of the key tumor suppressor *Brca1* (Beger et al., 2001) and also suppresses miR335, a positive regulator of *Brca1* (Heyn et al., 2011). In the context of breast cancer, overexpression of Id4 tightly correlates with the 'triple-negative' subtype (de Candia et al., 2006; Wen et al., 2012) and inversely correlates with expression of BRCA1 and estrogen receptor α (ERα; Esr1) (Molyneux et al., 2010; Roldán et al., 2006).

There is mounting evidence that transcriptional regulators are essential for control of the mammary epithelial differentiation hierarchy (Visvader, 2009). As Id4 had been previously identified as a marker of the mammary stem (MaSC)/basal cell population (Dong et al., 2011; Lim et al., 2010), we generated a floxed Id4 mouse model to permit further analysis of the role of Id4 in mammopoiesis, in the absence of the early lethality that accompanies germline deletion of this gene. Here, we report a dual role for Id4 in regulation of the estrogen-signaling axis in both the developing mammary gland and ovary.

RESULTS AND DISCUSSION

Conditional deletion of Id4 results in a delay in mammary gland morphogenesis

To generate a conditionally targeted *Id4* mouse model, the entire open reading frame of *Id4* located in exons 1 and 2 was flanked with *LoxP* sites. A GFP reporter cassette enabled tracking of specific cell populations and proved to be a sensitive read-out of *Id4* promoter activity (Fig. 1A,B; supplementary material Fig. S1A). FACS (fluorescence-activated cell sorting) analysis of GFP at different developmental time-points showed that endogenous Id4 expression was highest in the MaSC/basal population ($CD29^{hi}CD24^{+}$) (Shackleton et al., 2006) at puberty (supplementary material Fig. S1B), consistent with previous gene profiling studies (Lim et al., 2010). Id4 may be expressed in multiple basal cell types, as this subset contains stem cells, progenitors and myoepithelial cells. Unexpectedly, a small population of luminal cells was found to express Id4-GFP (Fig. 1B). Using CD49b for further fractionation, these GFP^{+} cells were identified as luminal progenitors ($CD29^{lo}CD24^{+}CD49b^{+}$) (Fig. 1C), and Id4 protein could also be demonstrated in this subset (supplementary material Fig. S1C). Immunostaining confirmed high Id4 expression in the outer myoepithelial layer of both the mammary ducts and terminal end buds (TEBs) at early puberty (supplementary material Fig. S1D,E).

To assess the *in vivo* effects of deleting *Id4* in mammary epithelial cells, we used two *cre* models, MMTV-*cre* or Keratin14-*cre*, both of

[1]ACRF Stem Cells and Cancer Division, Walter and Eliza Hall Institute of Medical Research, Parkville, Victoria 3052, Australia. [2]Department of Medical Biology, The University of Melbourne, Parkville, Victoria 3010, Australia. [3]Ovarian Biology Laboratory, Prince Henry's Institute, Monash Medical Center, Clayton, Victoria 3168, Australia. [4]Department of Anatomy and Developmental Biology, Monash University, Clayton, Victoria 3168, Australia. [5]Department of Medicine, The University of Melbourne, Parkville, Victoria 3010, Australia. [6]Department of Medical Oncology, The Royal Melbourne Hospital, Parkville, Victoria 3050, Australia.

*Author for correspondence (visvader@wehi.edu.au)

Received 29 January 2014; Accepted 4 June 2014

Development (2014) 141, 3159-3164 doi:10.1242/dev.108498

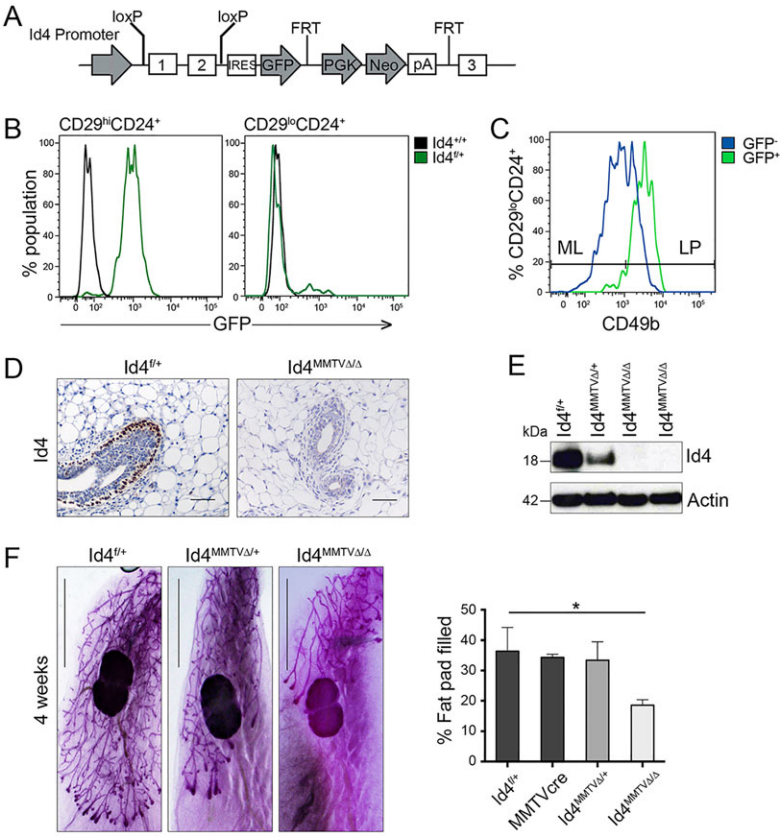

Fig. 1. MMTV-*cre* mediated deletion of Id4 curtails ductal elongation and branching. (A) Schematic of the floxed *Id4* allele. *LoxP* sites flank exons 1 and 2 that encode *Id4*. (B) FACS analysis of mammary glands from $Id4^{f/+}$ mice showing GFP expression in the basal ($CD29^{hi}CD24^{+}$) and luminal ($CD29^{lo}CD24^{+}$) populations (n=6 mice). (C) FACS analysis of GFP^{+} and GFP^{-} luminal populations using CD49b to identify mature luminal (ML) and luminal progenitor (LP) cells (n=6 mice). (D) Immunostaining for Id4 expression in mammary sections from 6-week-old virgin $Id4^{f/+}$ and MMTV-cre/$Id4^{f/f}$ ($Id4^{MMTV\Delta/\Delta}$) mice. Scale bars: 25 µm. (E) Western blot analysis of Id4 in 6-week-old virgin $Id4^{f/+}$, $Id4^{MMTV\Delta/+}$ and $Id4^{MMTV\Delta/\Delta}$ glands (n=2 independent mice). Actin provided the protein loading control. (F) Whole-mount glands from 4-week-old virgin $Id4^{f/+}$, MMTVcre, $Id4^{MMTV\Delta/+}$ and $Id4^{MMTV\Delta/\Delta}$ mice (n=3±s.d.). Scale bars: 0.5 cm.

which resulted in efficient recombination at the *Id4* locus (Fig. 1D,E; supplementary material Fig. S1F). The ductal elongation defects in MMTV-cre/$Id4^{f/f}$ and K14-cre/$Id4^{f/f}$ mammary glands recapitulated those previously described for germline knockout mice (Fig. 1F; supplementary material Fig. S1G) (Dong et al., 2011), with an intermediate phenotype observed for heterozygous mice. Although ductal elongation had been largely restored in MMTV-cre/$Id4^{f/f}$ glands by 8 weeks of age, complex branching of the ducts was still lacking (supplementary material Fig. S1H). To examine the repopulating capacity of *Id4*-deficient MaSCs isolated from mice at the onset of puberty when Id4 is prominently expressed in the TEBs, we transplanted the MaSC/basal population from early pubertal females. No difference in the frequency of repopulating units (Table 1) was evident for $Id4^{f/+}$ versus MMTV-cre/$Id4^{f/f}$ mice, indicating that Id4 was not required for MaSC function at this stage.

Deregulation of ERα in *Id4*-deficient mammary glands

The ductal architecture of *Id4*-deficient mammary ducts was unperturbed based on a range of lineage-specific markers, including the luminal markers keratin 8 (K8) and ERα (Fig. 2A). Surprisingly, $ER\alpha^{+}$ cells were more abundant in ductal cells of MMTV-cre/$Id4^{f/f}$ glands, relative to those of littermate controls (Fig. 2A,B). Immunostaining of freshly sorted, cytospun cells revealed that the proportion of $ER\alpha^{+}$ cells was increased in the luminal progenitor subset ($CD29^{lo}CD24^{+}CD49b^{+}$) from *Id4*-deficient mammary glands. Moreover, expression was also detected in the MaSC/basal population, which normally lacks expression of ER and PR (Fig. 2C,D; supplementary material Fig. S2A) (Asselin-Labat et al., 2006).

The expression of other proteins in the ERα pathway (Welboren et al., 2009), including FoxA1, the pioneering factor for ERα (Hurtado et al., 2011), and the progesterone receptor (PR) (Tanos et al., 2012) were next evaluated by immunostaining. Parallel to findings for ERα, FoxA1 mRNA and protein were dramatically upregulated in *Id4*-deficient MaSC/basal cells compared with those from control mice (Fig. 2E,F; supplementary material Fig. S2B). Moreover, the number of PR^{+} ductal cells nearly doubled in MMTV-cre/$Id4^{f/f}$ epithelium (supplementary material Fig. S2C). FACS analysis of Sca1 expression, an antigen linked to ER and PR expression (Shehata et al., 2012), also showed a significant increase in *Id4*-deficient luminal progenitor cells (supplementary material Fig. S2D). Thus, Id4 appears to have an important role in restraining expression of ERα and its associated network of transcription factors in basal and luminal cells.

Table 1. Limiting dilution analysis of the mammary repopulating frequency of the $CD29^{hi}CD24^{+}$ subset from 3-week-old $Id4^{f/+}$ and $Id4^{MMTV\Delta/\Delta}$ mice

	Number of positive outgrowths	
Number of cells injected per fat pad	$Id4^{f/+}$	$Id4^{MMTV\Delta/\Delta}$
100	14/20	14/27
200	17/20	19/22
400	19/20	10/11
Repopulating frequency	1/104	1/126
95% confidence interval	73.1-148	90-177
P value	0.432	

Id4-deficient ovaries express reduced levels of estrogen biosynthesis enzymes

Although ERα was aberrantly expressed in the basal and luminal epithelial subsets, no mammary hyperplasia was apparent in aged *Id4*-deficient mice. Mouse models in which ERα is overexpressed generally develop hyperplastic glands and adenocarcinomas with a short latency (Frech et al., 2005; Tilli et al., 2003). We therefore

Development (2014) 141, 3159-3164 doi:10.1242/dev.108498

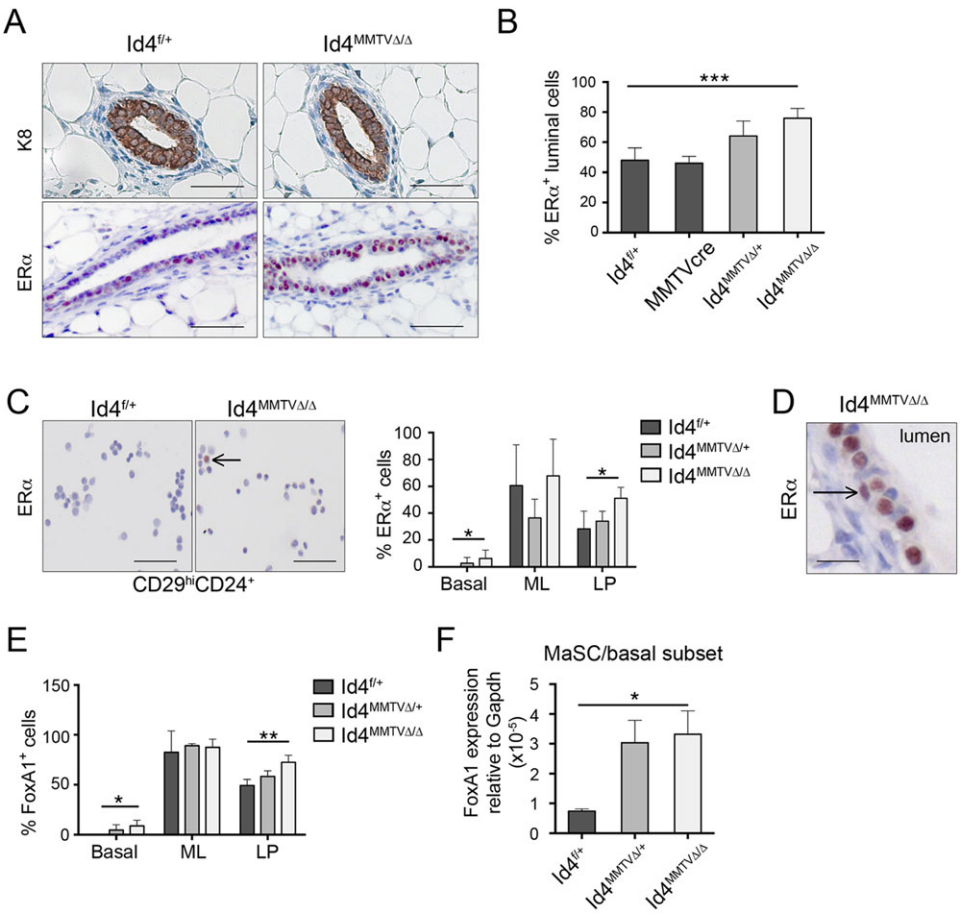

Fig. 2. Id4 loss results in ER pathway expression in myoepithelial cells. (A) Immunostaining of mammary gland sections from 6-week-old Id4$^{f/+}$ and Id4$^{MMTV\Delta/\Delta}$ mice for keratin 8 (K8) and ERα. Scale bars: 25 µm. (B) The proportion of luminal cells expressing ERα was quantified as a percentage of total luminal cells (*n*=6 mice±s.d.). (C) Immunostaining for ERα of sorted, cytospun cellular populations from 6-week-old virgin Id4$^{f/+}$ and Id4$^{MMTV\Delta/\Delta}$ mice: MaSC/basal (CD29^{hi}CD24^{+}), mature luminal (ML) (CD29^{lo}CD24^{+}CD49b^{-}) and luminal progenitor (LP) (CD29^{lo}CD24^{+}CD49b^{+}) subsets. Data for the MaSC/basal subset are shown (*n*=4 mice±s.d.). The arrow indicates an ERα-positive basal cell. Scale bars: 25 µm. (D) Immunostaining of mammary gland sections from 6-week-old virgin Id4$^{MMTV\Delta/\Delta}$ mice for ERα. The arrow indicates a myoepithelial cell expressing ERα. Scale bar: 5 µm. (E) Immunostaining of cytospun cell subsets for FoxA1 (*n*=4 mice±s.d.). (F) *Foxa1* mRNA levels in the MaSC/basal population from 6-week-old virgin Id4$^{f/+}$, Id4$^{MMTV\Delta/+}$ and Id4$^{MMTV\Delta/\Delta}$ mice (*n*=5 mice ±s.e.m.). Expression is relative to a *Gapdh* control.

hypothesized that estrogen production in MMTV-cre/Id4$^{f/f}$ mice might be compromised in *Id4*-deficient mice to account for the ductal elongation defects. Analysis of ovaries from these mice at estrus revealed irregular-shaped nodular ovaries that contained many large follicles in a loosely connected medulla (Fig. 3A). Pertinently, gene expression studies have identified Id4 expression in the estrogen-producing granulosa cells of the ovary (Hogg et al., 2010; Johnson et al., 2008), and expression of MMTV-*cre* has been reported in the oocyte and reproductive tract (Wagner et al., 2001). Indeed, immunostaining confirmed that Id4 was expressed within the granulosa cells of secondary and antral follicles of ovaries from control mice but was absent in MMTV-cre/Id4$^{f/f}$ ovaries (Fig. 3B; supplementary material Fig. S3A).

The number of secondary and antral follicles as well as atretic (degenerating) follicles was increased in the ovaries of MMTV-cre/Id4$^{f/f}$ mice, although the total number of follicles per ovary was comparable to that in control mice (Fig. 3C; supplementary material Fig. S3B). Increased responsiveness of granulosa cells to the pituitary hormone follicle-stimulating hormone (FSH) could account for the increased numbers of antral follicles. The elevated FSH-receptor transcript levels in *Id4*-deficient ovaries (Fig. 3D) are consistent with the increase in maturing follicle numbers and may mediate enhanced responsiveness to FSH.

Despite an overall increase in the number of growing and maturing follicles in the ovaries from *Id4*-deficient mice, we found that expression of key estrogen biosynthesis enzymes *Cyp11a1* (cholesterol side chain cleavage enzyme), *Star* (steroidogenic acute regulatory protein), *Cyp17a1* (17,20 lyase), *HSD3β* (3-β-hydroxysteroid dehydrogenase; *Hsd3b*) and *Cyp19a1* (aromatase) were all significantly lower in *Id4*-deficient ovaries relative to controls (Fig. 3E). Conversely, expression of the key negative transcriptional regulator of the majority of these enzymes, *Foxl2* (Escudero et al., 2010), was increased (Fig. 3F). In order to verify a reduction in estrogen production, we measured the weight of uteri. The uterus is extremely sensitive to estrogen levels and uterine weight is commonly used as measure of estrogen response (Liew et al., 2010). Notably, the wet uterus weights of *Id4*-deficient mice were significantly reduced compared with control mice (Fig. 3G), indicating diminished levels of circulating estrogen and an important role for Id4 in ovarian development.

To investigate whether the delayed ductal elongation in *Id4*-deficient mammary glands was a consequence of lower levels of systemic estrogen, we performed an estrogen-replacement experiment (supplementary material Fig. S3C). Using a regimen similar to that previously described (Gresack and Frick, 2006), we increased the amount of circulating estrogen in female mice during pubertal development and verified the increase via uterine wet weight measurements (supplementary material Fig. S3D). Importantly, ductal morphogenesis was rescued in MMTV-cre/Id4$^{f/f}$ females injected with estrogen, implying that these defects are not intrinsic to the mammary epithelium and likely result from low circulating estrogen levels (supplementary material Fig. S3E). The increase in ERα-positive luminal cells was still apparent in *Id4*-deficient mammary glands with higher circulating estrogen levels (Fig. 3H), suggesting that this effect is autonomous to the epithelium.

Reduced serum estrogen may account for the differences observed in the mammary repopulating frequencies for 12- to 16-week-old *Id4*$^{-/-}$ (Dong et al., 2011) versus young MMTV-cre/Id4$^{f/f}$ mice (Table 1). Stem cells isolated from older mice have likely been

Development (2014) 141, 3159-3164 doi:10.1242/dev.108498

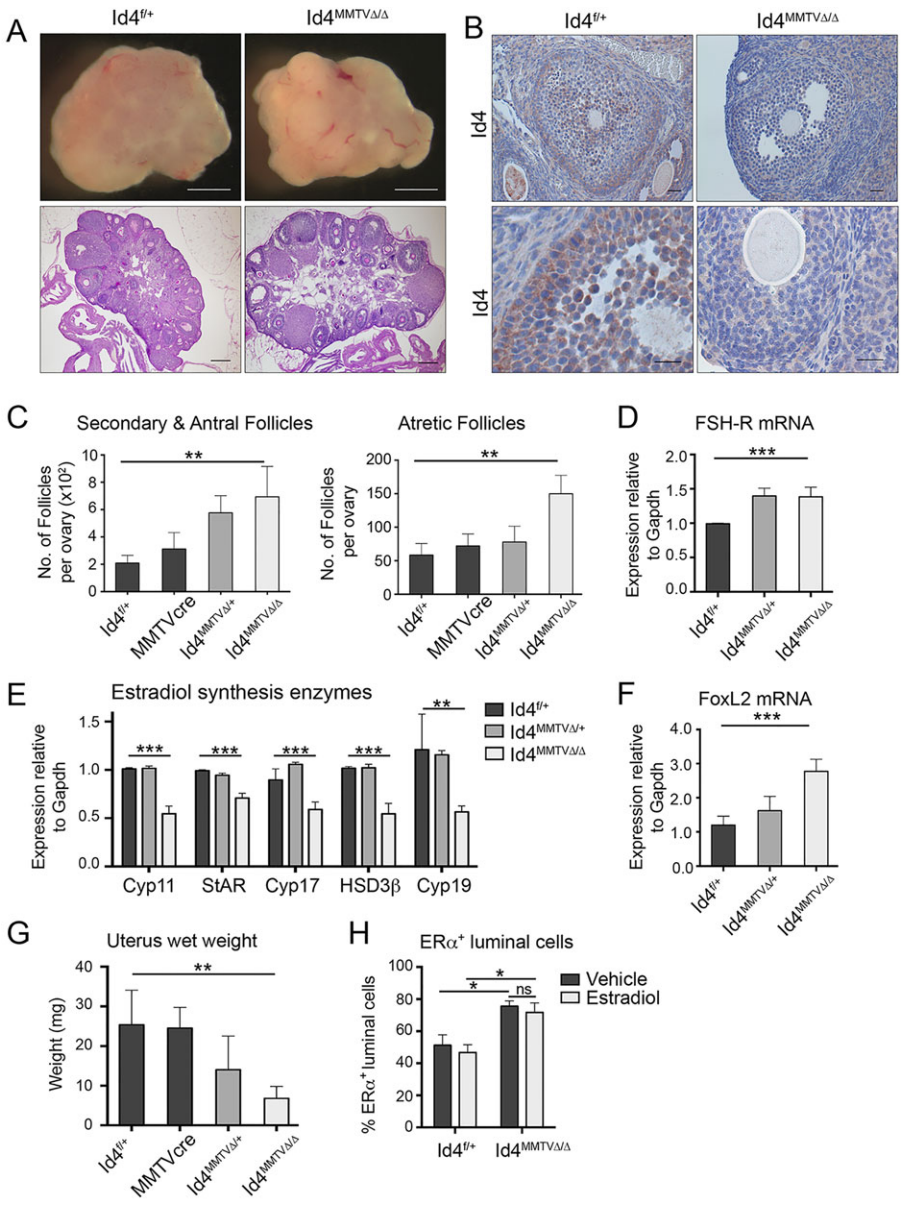

Fig. 3. *Id4* deficiency impacts ovarian follicle maturation and estrogen production. (A) Whole ovaries and sections from Id4$^{f/+}$ and Id4$^{MMTV\Delta/\Delta}$ mice taken at the estrus stage. Scale bars: 0.5 mm (whole ovary); 0.2 mm (sections). (B) Immunostaining for Id4 in Id4$^{f/+}$ and Id4$^{MMTV\Delta/\Delta}$ follicles. Scale bars: 25 µm. (C) The numbers of secondary and antral, and of atretic follicles per ovary were counted in 6-week-old virgin Id4$^{f/+}$, MMTVcre, Id4$^{MMTV\Delta/+}$ and Id4$^{MMTV\Delta/\Delta}$ mice (n=3 mice±s.d.). (D) Expression analysis of *Fshr* mRNA. (E,F) Analysis of mRNA levels of estradiol synthesis enzymes: *Cyp11*, *Star*, *Cyp17*, *HSD3β* and *Cyp19* (E), and *Foxl2* (F) in whole ovaries from 6-week-old virgin Id4$^{f/+}$, Id4$^{MMTV\Delta/+}$ and Id4$^{MMTV\Delta/\Delta}$ mice. (G) Wet weight measurements for uteri from 6-week-old Id4$^{f/+}$, MMTVcre, Id4$^{MMTV\Delta/+}$ and Id4$^{MMTV\Delta/\Delta}$ mice staged at either estrus or proestrus. (D-G) n=3 mice per genotype±s.d. at estrus stage. (H) Quantitation of ERα$^+$ ductal cells in an estradiol-replacement experiment; Id4$^{f/+}$ mice are compared with Id4$^{MMTV\Delta/\Delta}$ mice treated with either vehicle or estradiol (n=4 mice±s.e.m.). *P<0.05; **P<0.01; ***P<0.001 (Student's t-test).

exposed to a low-estrogen environment for several weeks prior to transplantation, whereas this will not apply to young pubertal mice. Indeed, MaSCs from ovariectomized females show significantly reduced activity (Asselin-Labat et al., 2010).

Id4 negatively regulates ERα protein expression

To determine whether Id4 directly targets the *Esr1* gene in mammary epithelial cells, we performed chromatin immunoprecipitation (ChIP) analysis of endogenous Id4 protein in both primary sorted luminal cells and the CommaDβgeo cell line. Specific binding of Id4 occurred at a region located 5.9 kb upstream of the ERα promoter (Fig. 4A; supplementary material Fig. S3F). We presume that Id4 binds the ERα upstream regulatory region as part of a larger protein complex, as Id4 itself cannot bind to DNA. Furthermore, an Id4 site was identified 8.3 kb upstream of the *Foxa1* transcription start site, and perhaps forms part of a similar protein complex (Fig. 4B; supplementary material Fig. S3G). To further explore a transcriptional link between Id4 and ERα, we overexpressed Id4 in CommaDβgeo cells. Western blot analysis showed a consistent decrease in ERα protein expression in cells overexpressing the MSCV-Id4 construct compared with control cells (Fig. 4C), thus invoking a direct link between Id4 and ERα expression. In the context of tumorigenesis, although little difference in tumor latency was observed between Id4$^{f/+}$/Wnt1 and K14-cre/Id4$^{f/f}$/Wnt1 mice (data not shown), *Id4*-deficient tumors expressed high levels of ERα and FoxA1 (Fig. 4D). As Wnt1 tumors express high levels of Id4 and have a signature reminiscent of the MaSC/basal population (ERα and FoxA1 negative) (Lim et al., 2010), these data underscore the importance of Id4 in regulation of the ER pathway.

In summary, our findings have revealed an unsuspected role for Id4 in negatively regulating ERα expression in basal and luminal cells of the mammary gland and in controlling the expression of key estrogen biosynthesis enzymes in the ovary. The independent role of Id4 in follicle development in the ovary likely results in reduced estrogen levels in *Id4*-deficient mice with consequent effects on mammary gland development.

MATERIALS AND METHODS

Mice

Floxed-Id4 mice were generated by Ozgene; MMTV-*cre* (line A) mice were a gift from K.-U. Wagner (University of Nebraska Medical Center, USA);

Development (2014) 141, 3159-3164 doi:10.1242/dev.108498

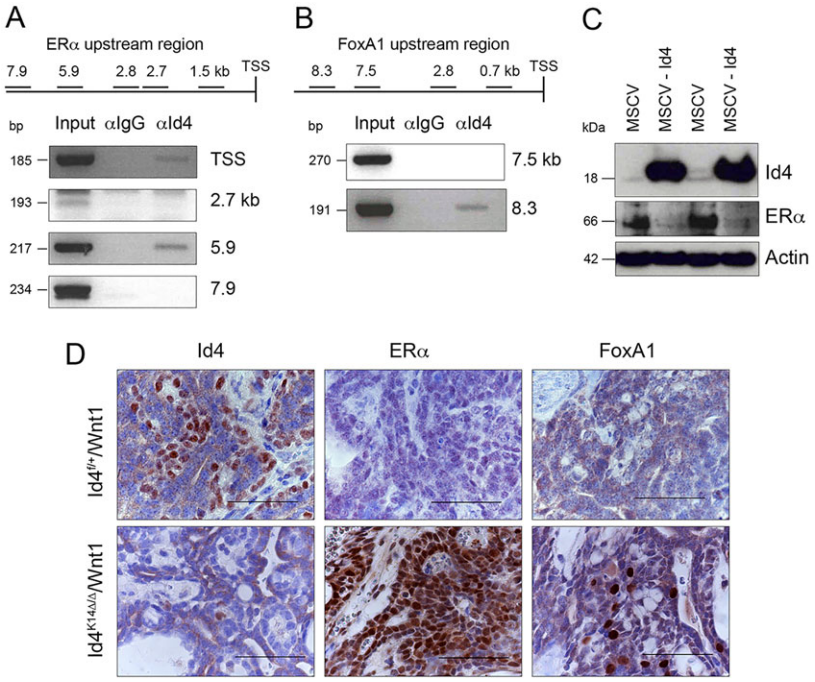

Fig. 4. Id4 negatively regulates expression of ERα. (A) ChIP analysis of Id4 on the *ERα* promoter region in luminal ($CD29^{lo}CD24^{+}$) cells: input and immunoprecipitation with IgG or Id4 antibody on promoter regions 2.7, 5.9 and 7.9 kb upstream of the transcription start site (TSS). (B) ChIP analysis of Id4 on the *Foxa1* promoter region in luminal cells: input and immunoprecipitation with IgG or Id4 antibody on promoter regions 7.5 and 8.3 kb upstream of the TSS. (C) Overexpression of Id4 in CommaDβgeo cells. Western blot analysis of Id4, ERα and actin expression in control cells transduced with Id4 or an empty vector. (D) Immunostaining of sections from $Id4^{f/+}$/Wnt1 and $Id4^{K14\Delta/\Delta}$/Wnt1 tumors for Id4, ERα and FoxA1 expression. Scale bars: 25 µm.

K14-*cre* mice were a gift from J. Jonkers (Netherlands Cancer Institute, The Netherlands). MMTV-*cre* and K14-*cre* mice were maintained on a FVB/N background and floxed-Id4 mice were analyzed on a mixed FVB/N C57/Bl6 background. All animal experiments conform to regulatory standards and were approved by the Walter and Eliza Hall Institute (WEHI) Animal Ethics Committee. Vaginal smears were taken with saline and counterstained with Hematoxylin and Eosin. Uterus wet weight measurements taken from single horn (proestrus or estrus), with adipose and ovary removed.

17β-Estradiol (Sigma-Aldrich) in ethanol was diluted in sunflower seed oil (Sigma-Aldrich) to 4 µl/g for subcutaneous injection into mice at 0.2 mg/kg body weight. Mouse tail DNA was genotyped using primers (shown in supplementary material Table S1) under the following cycling conditions: 95°C for 5 min; 35 cycles of 95°C for 1 min, 60°C for 1 min and 72°C for 1.5 min; 72°C for 5 min.

Histology and immunohistochemistry

Inguinal mammary glands fixed in Carnoy's solution overnight were stained in Carmine Alum. Whole-mounts were quantified using ImageJ software (Softonic). Mammary glands or ovaries were fixed in 4% paraformaldehyde and embedded in paraffin wax. Sections (5 µm) were immunostained with antibodies in supplementary material Table S2 using standard protocols. For immunohistochemistry, antibodies and ABC reagent (Vector Laboratories) were incubated for 30 min at room temperature. For immunofluorescence, primary antibodies were incubated at 4°C overnight and secondary antibodies for 30 min at room temperature.

Follicle counts were obtained as previously described (Kerr et al., 2006; Myers et al., 2004), counted on an Olympus BX50 microscope with an Autoscan stage (Autoscan Systems) and a CASTGRID stereological system (Olympus). Atretic follicle counts used the fractionator/physical dissector method as previously described (Myers et al., 2004). Antral follicles were considered atretic if more than 10% of primordial, primary or secondary follicle granulosa cells were apoptotic or contained a degenerating oocyte.

Flow cytometry

Fresh inguinal and thoracic mammary glands were dissected and single cell suspensions generated as described previously (Shackleton et al., 2006). Data were collected and cells sorted on FACS ARIA II (Becton Dickinson) and analyzed using FlowJo software.

Transplantation assays into 3-week-old recipient mice and limiting dilution analysis have been described (Shackleton et al., 2006). Outgrowths were examined 8 weeks post-transplantation.

Cells were spun down onto Superfrost Plus-coated slides using the Thermo Cytospin machine (Thermo Fisher Scientific) at 160 ***g*** for 3 min, fixed in 4% paraformaldehyde and stored in 70% ethanol prior to immunohistochemistry.

Quantitative RT-PCR

RNA was extracted from ground tissues using QIAshredder columns (Qiagen) prior to using the RNeasy RNA extraction kit (Qiagen), according to the manufacturer's instructions. qRT-PCR was performed on cDNA using SYBRGreen (Bioline) on the Corbett RotorGene qPCR machine and software (Life Technologies). Primers are listed in supplementary material Table S1.

ChIP and western blot analyses

ChIP was performed on CommaDβGeo cells and freshly sorted C57BL/6 luminal cells as described previously (Voss et al., 2012). Shearing was performed to generate ∼500 bp fragments. PCR primers are listed in supplementary material Table S1.

MSCV-Id4-dsRed and control constructs (a generous gift from A. Swarbrick, Garvan Institute of Medical Research, Australia) were transduced into CommaDβgeo cells using retrovirus produced in Phoenix cells. Bright Ds-Red cells were sorted 48 h post-infection for western blot analysis. Fresh mammary glands were snap-frozen, pulverized in liquid nitrogen and lysed in KalbC lysis buffer for western blotting as previously described (Asselin-Labat et al., 2007).

Statistics

Statistical analysis was performed using GraphPad Prism software (GraphPad Software) using Student's *t*-test. Significance is indicated on the figures using the following convention: $*P<0.05$; $**P<0.01$; $***P<0.001$.

Acknowledgements

We are grateful to J. Findlay for helpful discussions, and to the Animal, FACS and Histology facilities at WEHI.

Competing interests

The authors declare no competing financial interests.

Author contributions

S.A.B. performed the majority of experiments and data analysis. S.A.B., J.E.V., K.J.H. and G.J.L. designed experiments. J.E.V. and G.J.L. conceptualized the

study. F.V. performed fat pad transplantations. N.Y.F. performed validation experiments on the targeted model. L.H. performed ovary dissection. S.H.L., K.J.H. and C.L.S. discussed and performed follicle analysis and counts. S.A.B. and J.E.V. wrote the manuscript.

Funding

This work was supported by the Australian National Health and Medical Research Council (NHMRC) [461221 and 1016701 NHMRC IRIISS]; by the Victorian State Government through VCA funding of the Victorian Breast Cancer Research Consortium and Operational Infrastructure Support; and by the Australian Cancer Research Foundation. S.A.B. was supported by an NHMRC Postgraduate Scholarship [1017256]. K.J.H. and G.J.L. were supported by NHMRC Fellowships [1050130 and 637307, respectively]. N.Y.F. was supported by an NBCF Postdoctoral Fellowship. C.L.S. was supported by the Cancer Council Victoria (Sir Edward Dunlop Fellowship in Cancer Research) and by the Victorian Cancer Agency (Clinical Fellowship). J.E.V. was supported by an Australia Fellowship.

Supplementary material

Supplementary material available online at
http://dev.biologists.org/lookup/suppl/doi:10.1242/dev.108498/-/DC1

References

Asselin-Labat, M.-L., Shackleton, M., Stingl, J., Vaillant, F., Forrest, N. C., Eaves, C. J., Visvader, J. E. and Lindeman, G. J. (2006). Steroid hormone receptor status of mouse mammary stem cells. *J. Natl. Cancer Inst.* **98**, 1011-1014.

Asselin-Labat, M.-L., Sutherland, K. D., Barker, H., Thomas, R., Shackleton, M., Forrest, N. C., Hartley, L., Robb, L., Grosveld, F. G., van der Wees, J. et al. (2007). Gata-3 is an essential regulator of mammary-gland morphogenesis and luminal-cell differentiation. *Nat. Cell Biol.* **9**, 201-209.

Asselin-Labat, M.-L., Vaillant, F., Sheridan, J. M., Pal, B., Wu, D., Simpson, E. R., Yasuda, H., Smyth, G. K., Martin, T. J., Lindeman, G. J. et al. (2010). Control of mammary stem cell function by steroid hormone signalling. *Nature* **465**, 798-802.

Bedford, L., Walker, R., Kondo, T., van Crüchten, I., King, E. R. and Sablitzky, F. (2005). Id4 is required for the correct timing of neural differentiation. *Dev. Biol.* **280**, 386-395.

Beger, C., Pierce, L. N., Kruger, M., Marcusson, E. G., Robbins, J. M., Welcsh, P., Welch, P. J., Welte, K., King, M.-C., Barber, J. R. et al. (2001). Identification of Id4 as a regulator of BRCA1 expression by using a ribozyme-library-based inverse genomics approach. *Proc. Natl. Acad. Sci. USA* **98**, 130-135.

de Candia, P., Akram, M., Benezra, R. and Brogi, E. (2006). Id4 messenger RNA and estrogen receptor expression: inverse correlation in human normal breast epithelium and carcinoma. *Hum. Pathol.* **37**, 1032-1041.

Dong, J., Huang, S., Caikovski, M., Ji, S., McGrath, A., Custorio, M. G., Creighton, C. J., Maliakkal, P., Bogoslovskaia, E., Du, Z. et al. (2011). ID4 regulates mammary gland development by suppressing p38MAPK activity. *Development* **138**, 5247-5256.

Escudero, J. M., Haller, J. L., Clay, C. M. and Escudero, K. W. (2010). Microarray analysis of Foxl2 mediated gene regulation in the mouse ovary derived KK1 granulosa cell line: over-expression of Foxl2 leads to activation of the gonadotropin releasing hormone receptor gene promoter. *J. Ovarian Res.* **3**, 4.

Frech, M., Halama, E., Tilli, M., Singh, B., Gunther, E., Chodosh, L., Flaws, J. and Furth, P. (2005). Deregulated estrogen receptor α expression in mammary epithelial cells of transgenic mice results in the development of ductal carcinoma in situ. *Cancer Res.* **65**, 681-685.

Gresack, J. E. and Frick, K. M (2006). Effects of continuous and intermittent estrogen treatments on memory in aging female mice. *Brain Res.* **1115**, 135-147.

Heyn, H., Engelmann, M., Schreek, S., Ahrens, P., Lehmann, U., Kreipe, H., Schlegelberger, B. and Beger, C. (2011). MicroRNA miR-335 is crucial for the BRCA1 regulatory cascade in breast cancer development. *Int. J. Cancer* **129**, 2797-2806.

Hogg, K., Etherington, S. L, Young, J. M., McNeilly, A. S. and Duncan, W. C. (2010). Inhibitor of differentiation (Id) genes are expressed in the steroidogenic cells of the ovine ovary and are differentially regulated by members of the transforming growth factor-β family. *Endocrinology* **151**, 1247-1256.

Hurtado, A., Holmes, K. A., Ross-Innes, C. S., Schmidt, D. and Carroll, J. S. (2011). FOXA1 is a key determinant of estrogen receptor function and endocrine response. *Nat. Genet.* **43**, 27-33.

Johnson, A. L., Haugen, M. J. and Woods, D. C. (2008). Role for inhibitor of differentiation/deoxyribonucleic acid-binding (Id) proteins in granulosa cell differentiation. *Endocrinology* **149**, 3187-3195.

Kerr, J. B., Duckett, R., Myers, M., Britt, K. L., Mladenovska, T. and Findlay, J. K. (2006). Quantification of healthy follicles in the neonatal and adult mouse ovary: evidence for maintenance of primordial follicle supply. *Reproduction* **132**, 95-109.

Lasorella, A., Benezra, R. and Iavarone, A. (2014). The ID proteins: master regulators of cancer stem cells and tumour aggressiveness. *Nat. Rev. Cancer* **14**, 77-91.

Liew, S. H., Drummond, A. E., Jones, M. E. and Findlay, J. K. (2010). The lack of estrogen and excess luteinizing hormone are responsible for the female ArKO mouse phenotype. *Mol. Cell. Endocrinol.* **327**, 56-64.

Lim, E., Wu, D., Pal, B., Bouras, T., Asselin-Labat, M.-L., Vaillant, F., Yagita, H., Lindeman, G. J., Smyth, G. K. and Visvader, J. E. (2010). Transcriptome analyses of mouse and human mammary cell subpopulations reveal multiple conserved genes and pathways. *Breast Cancer Res.* **12**, R21.

Molyneux, G., Geyer, F. C., Magnay, F.-A., McCarthy, A., Kendrick, H., Natrajan, R., MacKay, A., Grigoriadis, A., Tutt, A., Ashworth, A. et al. (2010). BRCA1 basal-like breast cancers originate from luminal epithelial progenitors and not from basal stem cells. *Cell Stem Cell* **7**, 403-417.

Myers, M., Britt, K. L., Wreford, N. G. M., Ebling, F.J. P. and Kerr, J. B. (2004). Methods for quantifying follicular numbers within the mouse ovary. *Reproduction* **127**, 569-580.

Roldán, G., Delgado, L. and Musé, I. M. (2006). Tumoral expression of BRCA1, estrogen receptor alpha and ID4 protein in patients with sporadic breast cancer. *Cancer Biol. Ther.* **5**, 505-510.

Shackleton, M., Vaillant, F., Simpson, K. J., Stingl, J., Smyth, G. K., Asselin-Labat, M.-L., Wu, L., Lindeman, G. J. and Visvader, J. E. (2006). Generation of a functional mammary gland from a single stem cell. *Nature* **439**, 84-88.

Sharma, P., Knowell, A., Chinaranagari, S., Komaragiri, S., Nagappan, P., Patel, D., Havrda, M. C. and Chaudhary, J. (2013). Id4 deficiency attenuates prostate development and promotes PIN-like lesions by regulating androgen receptor activity and expression of NKX3.1 and PTEN. *Mol. Cancer* **12**, 67.

Shehata, M., Teschendorff, A., Sharp, G., Novcic, N., Russell, I. A., Avril, S., Prater, M., Eirew, P., Caldas, C., Watson, C. J. et al. (2012). Phenotypic and functional characterisation of the luminal cell hierarchy of the mammary gland. *Breast Cancer Res.* **14**, R134.

Sikder, H. A., Devlin, M. K., Dunlap, S., Ryu, B. and Alani, R. M. (2003). Id proteins in cell growth and tumourigenesis. *Cancer Cell* **3**, 525-530.

Tanos, T., Rojo, L., Echeverria, P. and Brisken, C. (2012). ER and PR signaling nodes during mammary gland development. *Breast Cancer Res.* **14**, 210.

Tilli, M. T., Frech, M. S., Steed, M. E., Hruska, K. S., Johnson, M. D., Flaws, J. A. and Furth, P. A. (2003). Introduction of estrogen receptor-α into the tTA/TAg conditional mouse model precipitates the development of estrogen-responsive mammary adenocarcinoma. *Am. J. Pathol.* **163**, 1713-1719.

Visvader, J. (2009). Keeping abreast of the mammary epithelial hierarchy and breast tumorigenesis. *Genes Dev.* **23**, 2563-2577.

Voss, A. K., Dixon, M. P., McLennan, T., Kueh, A. J. and Thomas, T. (2012). Chromatin immunoprecipitation of mouse embryos. *Methods Mol. Biol.* **809**, 335-352.

Wagner, K.-U., Ward, T., Davis, B., Wiseman, R. and Hennighausen, L. (2001). Spatial and temporal expression of the Cre gene under the control of the MMTV-LTR in different lines of transgenic mice. *Transgenic Res.* **10**, 545-553.

Welboren, W.-J., Sweep, F. C. G. J., Span, P. and Stunnenberg, H. G. (2009). Genomic actions of estrogen receptor α: what are the targets and how are they regulated? *Endocr. Relat. Cancer* **16**, 1073-1089.

Wen, Y. H., Ho, A., Patil, S., Akram, M., Catalano, J., Eaton, A., Norton, L., Benezra, R. and Brogi, E. (2012). Id4 protein is highly expressed in triple-negative breast carcinomas: possible implications for BRCA1 downregulation. *Breast Cancer Res. Treat.* **135**, 93-102.

Yun, K., Mantani, A., Garel, S., Rubenstein, J. and Israel, M. A. (2004). Id4 regulates neural progenitor proliferation and differentiation in vivo. *Development* **131**, 5441-5448.

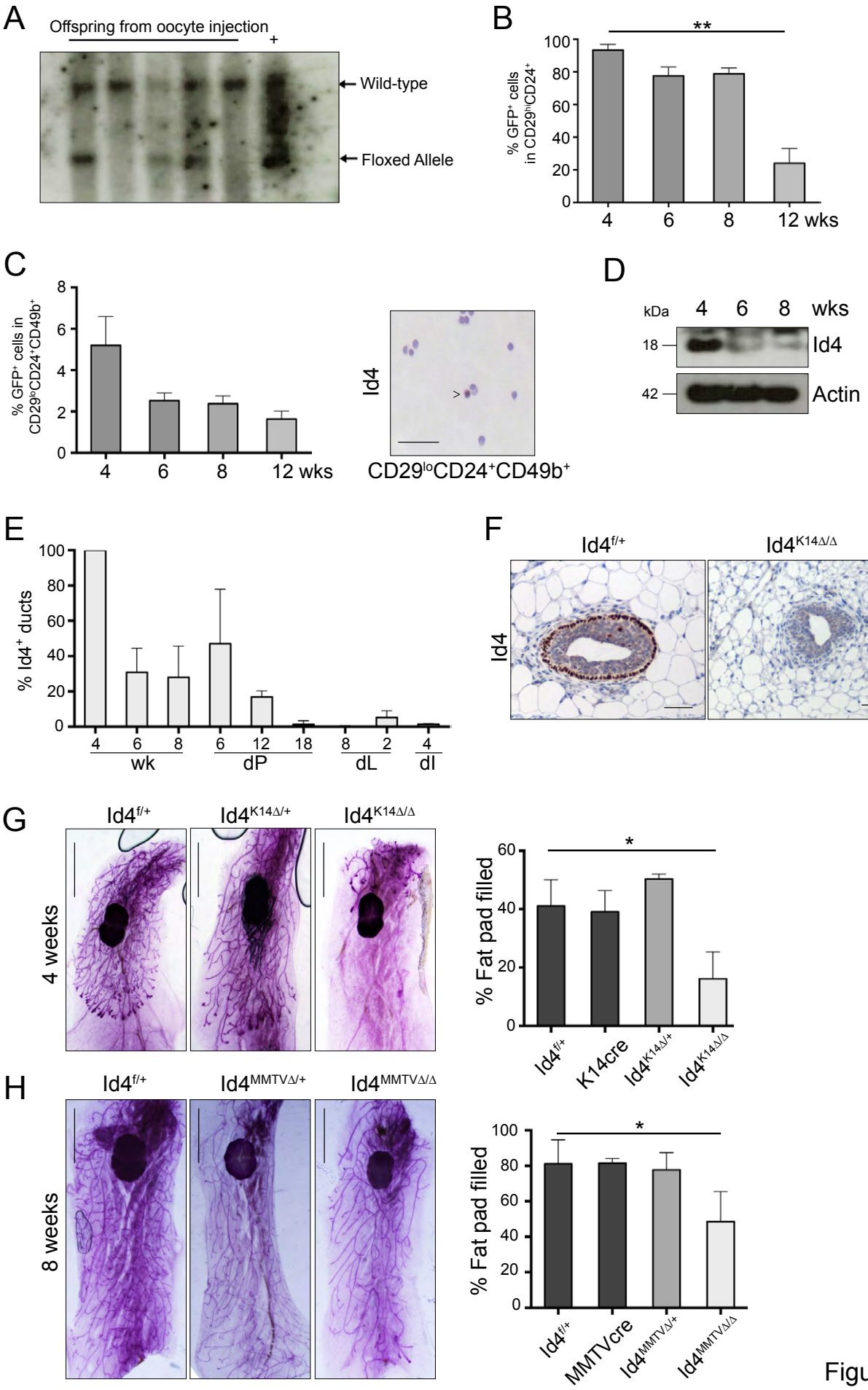
A
Offspring from oocyte injection
+
Wild-type
Floxed Allele
B
**
% GFP+ cells in CD29hiCD24+
100
80
60
40
20
0
4
6
8
12 wks
C
% GFP+ cells in CD29loCD24+CD49b+
8
6
4
2
0
4
6
8
12 wks
Id4
CD29loCD24+CD49b+
D
kDa
4
6
8
wks
18
Id4
42
Actin
E
% Id4+ ducts
100
80
60
40
20
0
4
6
8
6
12
18
8
2
4
wk
dP
dL
dl
F
Id4f/+
Id4K14Δ/Δ
Id4
G
Id4f/+
Id4K14Δ/+
Id4K14Δ/Δ
4 weeks
% Fat pad filled
60
40
20
0
*
Id4f/+
K14cre
Id4K14Δ/+
Id4K14Δ/Δ
H
Id4f/+
Id4MMTVΔ/+
Id4MMTVΔ/Δ
8 weeks
% Fat pad filled
100
80
60
40
20
0
*
Id4f/+
MMTVcre
Id4MMTVΔ/+
Id4MMTVΔ/Δ

Figure S1

Fig. S1. Id4 expression is highest in the mammary glands of pubertal mice. (A) Southern blot analysis to identify positive offspring carrying the wild-type and floxed *Id4* allele. Arrows indicate the wild-type and floxed alleles. (B) FACS analysis of GFP reporter expression in MaSC/basal ($CD29^{hi}CD24^{+}$) cells at 4, 6, 8 and 12 weeks-of-age (n = 3 mice ± s.e.m.). (C) FACS analysis of GFP reporter expression in luminal progenitor ($CD29^{lo}CD24^{+}CD49b^{+}$) cells at 4, 6, 8 and 12 weeks-of-age (n = 3 mice ± s.e.m.). Representative image of Id4 immunostaining of freshly sorted $CD29^{lo}CD24^{+}CD49b^{+}$ cells. The arrow indicates a positive cell. Scale bar, 25 μm. (D) Western blot showing Id4 expression in virgin mice at 4, 6 and 8 weeks-of-age. Actin provided the protein loading control. (E) Quantitation of Id4 immunohistochemical data at various time-points in virgin (wk), pregnant (dP), lactating (L) and involuting (I) mice. The percentage of Id4-positive ducts is shown as a proportion of total ducts per section (virgin) or per field of view (pregnancy, lactation, involution) (n = 3 mice ± s.e.m.). (F) Immunostaining of sections from 6 week-old virgin $Id4^{f/+}$ and $Id4^{K14\Delta/\Delta}$ mice for Id4. Scale bar, 25 μm. (G) Whole-mount of representative mammary glands from 4 week-old virgin $Id4^{f/+}$, K14cre, $Id4^{K14\Delta/+}$ and $Id4^{K14\Delta/\Delta}$ mice (n = 3 mice ± s.d.). (H) Extent of fat pad filling in 8 week-old $Id4^{f/+}$, MMTVcre, $Id4^{MMTV\Delta/+}$ and $Id4^{MMTV\Delta/\Delta}$ mammary glands, quantified as a percentage of total fat pad (n = 3 mice ± s.d.).

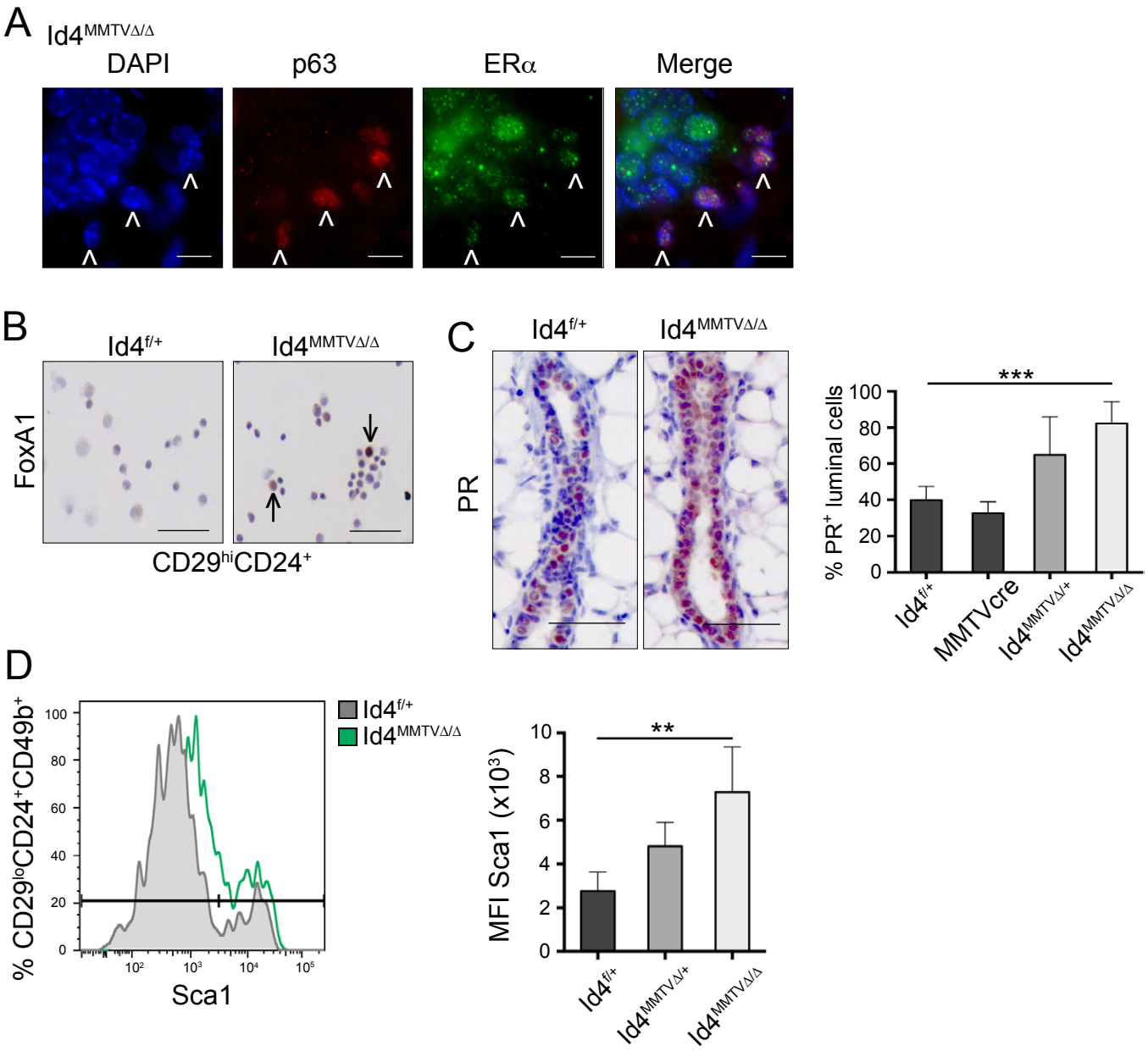

Fig. S2. *Id4*-deficiency affects the luminal population. (A) Co-staining of p63, ERα and DAPI on 6 week-old Id4$^{MMTV\Delta/\Delta}$ mammary sections. Arrows indicate basal cells expressing both p63 and ERα in a representative duct. (B) FoxA1 immunostaining on sorted, cyto-spun MaSC/basal cells (CD29^{hi}CD24^{+}) from 6 week-old Id4$^{f/+}$ and Id4$^{MMTV\Delta/\Delta}$ mice (n = 4 mice). Scale bar, 25 µm. (C) Immunostaining for Progesterone Receptor (PR) expression on sections from 6 week-old Id4$^{f/+}$ and Id4$^{MMTV\Delta/\Delta}$ mice. Bar graph indicates percent PR-positive ductal cells depicted as a proportion of total ductal cells for Id4$^{f/+}$, MMTVcre, Id4$^{MMTV\Delta/+}$ and Id4$^{MMTV\Delta/\Delta}$ mice (n = 7 mice ± s.d.). (D) FACS analysis of Sca1 expression in the luminal progenitor population (CD29^{lo}CD24^{+}CD49b^{+}) of 6 week-old Id4$^{f/+}$ and Id4$^{MMTV\Delta/\Delta}$ mice. Bar graph indicates the mean fluorescence intensity (MFI) of Sca1 in the luminal population of 6 week-old Id4$^{f/+}$, Id4$^{MMTV\Delta/+}$ and Id4$^{MMTV\Delta/\Delta}$ mice (n = 4 mice ± s.d.).

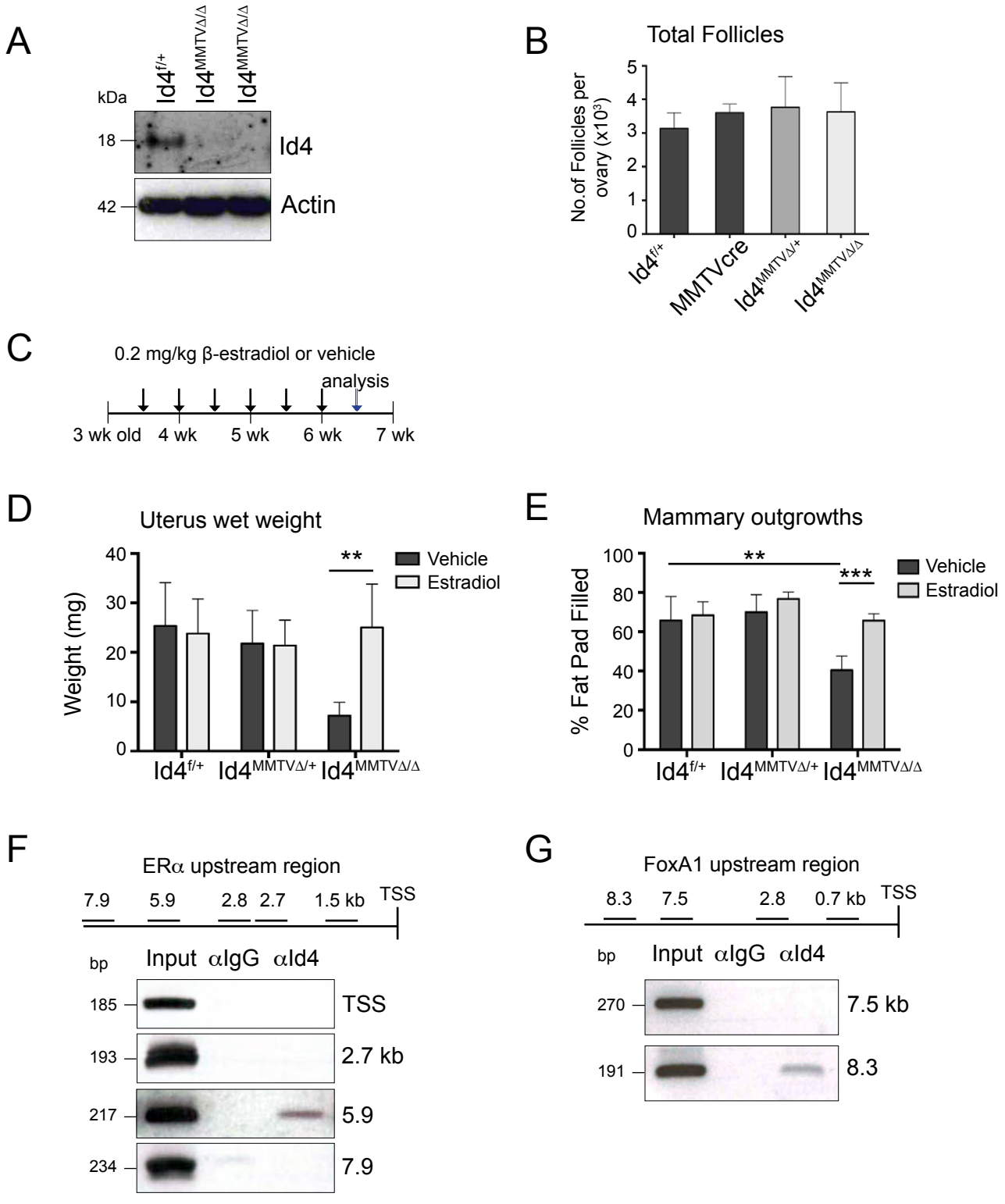

Fig. S3. Exogenous β-estradiol rescues ductal elongation defects in *Id4*-deficient mammary glands. (A) Western blot analysis of Id4 expression in whole ground ovaries from 6 week-old $Id4^{f/+}$ and $Id4^{MMTV\Delta/\Delta}$ mice. Actin provides the loading control. (B) Analysis of the total number of follicles per ovary in 6 week-old $Id4^{f/+}$, MMTVcre, $Id4^{MMTV\Delta/+}$ and $Id4^{MMTV\Delta/\Delta}$ mice (n = 3 mice ± s.e.m.). (C) Schematic diagram showing days of treatment with β-estradiol: 0.2 mg/kg β-estradiol or vehicle were injected twice per week over three weeks. Mammary glands and ovaries were collected at 6.5 weeks of age for analysis. (D) Uterus wet weight in $Id4^{f/+}$, $Id4^{MMTV\Delta/+}$ and $Id4^{MMTV\Delta/\Delta}$ mice in the vehicle and estradiol-treated arms at proestrus and estrus (n = 4 mice ± s.d.). (E) Fat pad filling by the mammary ductal tree for $Id4^{f/+}$, $Id4^{MMTV\Delta/+}$ and $Id4^{MMTV\Delta/\Delta}$ mice in the vehicle and estradiol-treated arms (n = 4 mice ± s.d.). (F) ChIP analysis of Id4 binding on the *ERα* promoter region in CommaDβgeo cells. Input and immuno-precipitations with IgG or Id4 antibody on promoter regions 2.7, 5.9 and 7.9 kb upstream of the TSS (n = 2). (G) ChIP analysis of Id4 binding on the *FoxA1* promoter region in CommaDβgeo cells. Input and immuno-precipitations with IgG or Id4 antibody on promoter regions 7.5 and 8.3 kb upstream of TSS (n = 2).

Table S1. List of primers for genotyping, qRT-PCR analysis and ChIP-PCR

Name	Sequence 5' to 3'	Product Length
MMTVcre Genotyping	CATCACTCGTTGCATCGACC CTGATCTGAGCTCTGAGTG	Transgene: 280 bp
K14cre Genotyping	CGATGCAACGCGTGATGAGGTTC GCACGTTCACCGGCATCAAC	Transgene: 350 bp
Id4 floxed Genotyping	GAGCAGCTCTCCGGTCGATTTCTG GGCTGCCGAGCCACCCAGGCTGTGG	WT: 269 bp Floxed: 320 bp
GAPDH qPCR	TGACATCAAGAAGGTGGTGAAGC AAGGTGGAAGAGTGGGAGTTGCTG	117 bp
ERalpha qPCR	CTGTCGGCTGCGCAAGTGTT CATCTCTCTGACGCTTGTGCT	101 bp
FoxA1 qPCR	GCTGGCTCCAGGATGTTAGGGAC GCTGACAGGGACAGAGGAGTAGG	108 bp
FSH-R qPCR	ACCGCTTGAAAAAGCTCCCT GTTCAGAGGTTTGCCGCCTC	114 bp
FoxL2 qPCR	AGCCGGCTTTTGTCATGATGG TACTGGTAGATGCCGGACAGA	250 bp
Cyp11 qPCR	ACATGGCCAAGATGGTACAGTTG ACGAAGCACCAGGTCATTCAC	119 bp
StAR qPCR	CGGGTGGATGGGTCAAGTTC CCAAGCGAAACACCTTGCC	230 bp
Cyp17 qPCR	TGACCAGTATGTAGGCTTCAGTCG TCCTTCGGGATGGCAAACTCTC	171 bp
HSD3β qPCR	TGGACAAAGTATTCCGACCAGA GGCACACTTGCTTGAACACAG	250 bp
Cyp19 qPCR	TGGAGAACAATTCGCCCTTTC TGGTTTGATGAGGAGAGCTTGC	273 bp
TSS ER α ChIP	CCAGTCTGAAATGCAGAG GGCTCAGCAGTTCTTG	185 bp
2.7 kb upstream ER α ChIP	GAGAGGATGTGTGTGCTG GAAGCCAGCCTGATCTAC	193 bp
5.9 kb upstream ER α ChIP	CCCTCACAGAGATATCT CACAAAGGAAGTAAAAGG	217 bp
7.9 kb upstream ER α ChIP	CGCTTGCTTCCTAGCCA GATCTCAGTCTTCTAGC	234 bp
7.5 kb upstream FoxA1 ChIP	CAACCTTCAGTCTCTCTC CTATTTCAGGAATGACG	270 bp
8.3 kb upstream FoxA1 ChIP	GCCCTCTTCTCTTGCAGGG GGGAAGACAGCTGTGCTC	191 bp

Table S2. List of antibodies for western blot, FACS analysis and immunohistochemistry

Antigen	Clone	Conjugate	Species	Supplier
Id4	82-12	Unconjugated	Rabbit	Biocheck
p63	4E5	Unconjugated	Mouse	AbCam
Keratin-8	-	Unconjugated	Mouse	Progen
ER α	MC-20	Unconjugated	Rabbit	Santa Cruz
PR	C-19	Unconjugated	Rabbit	Santa Cruz
FOXA1	-	Unconjugated	Rabbit	Abcam
β-Actin	AC-15	Unconjugated	Mouse	Sigma
Mouse IgG	-	HRP	Sheep	GE Healthcare
Rabbit IgG	-	HRP	Goat	GE Healthcare
Rabbit IgG	-	Biotin	Goat	Vector Laboratories
Mouse IgG	-	Biotin	Horse	Vector Laboratories
Rat IgG	-	Biotin	Goat	Vector Laboratories
Rabbit IgG	-	Alexa-647	Donkey	Life Technologies
Mouse IgG	-	Alexa-555	Donkey	Life Technologies
CD31	MEC 13.3	APC	Rat	BD Pharmingen
CD45	30-F11	APC	Rat	BD Pharmingen
TER-119	TER-119	APC	Rat	BD Pharmingen
CD24	M1/69	Pacific Blue	Rat	BioLegend
CD29	HMβ1-1	APCcy7	Hamster	BioLegend
CD49b	HMa2	Biotin	Hamster	eBioscience
CD61	HMβ3-1	APC	Hamster	Life Technologies
Sca1(Ly-6A/E)	E13-161.7	PE	Rat	BD Pharmingen
Streptavadin	-	Qdot-655	-	Life Technologies
Streptavadin	-	APCcy7	-	BD Pharmingen